

Ag/TiO₂ (Metal/Metal Oxide) Core Shell Nanoparticles for Biological Applications

D. Mangalaraj and D. Nithya Devi

Abstract This paper deals with the preparation of silver/titanium dioxide core shell nanoparticles using sobar method and the characterization of the prepared particles. The advantage of this method over the other available chemical methods is explained. Attempts have been made to employ the prepared particles to specific biological applications.

1 Introduction

Core/shell nanoparticles are gradually attracting more and more attention, since these nanoparticles have emerged at the frontier between materials chemistry and many other fields, such as electronics, biomedical, pharmaceuticals, optics and catalysis. Core shell nanoparticles are highly functional materials with modified properties. Sometimes properties arising from either core or shell materials can be quite different. The properties can be modified by changing either the constituting materials or the core to shell ratio. Because of the shell material coating, the properties of the core particle such as reactivity decrease or thermal stability can be modified, so that the overall particle stability and dispersibility of the core particle increases. The purpose of coating on the core particle are many fold, such as the surface modification, ability to increase the functionality, stability and dispersibility, control release of core, reduction in consumption of precious material. The majority of the core shell nanoparticles are used in biomedical field for bioimaging, controlled drug release, targeted drug delivery, cell labeling and tissue engineering application [1].

D. Mangalaraj (✉) · D. Nithya Devi
Department of Nanoscience and Technology, Bharathiar University,
Coimbatore 641046, India
e-mail: dmraj800@yahoo.com

2 Why Titanium Dioxide (TiO₂) and Silver (Ag) Nanoparticles?

Metal nanoparticles, with a high specific surface area and a high fraction of surface atoms, have been studied extensively due to their unique physico-chemical characteristics including catalytic activity, optical properties, electronic properties, antimicrobial activity and magnetic properties. Among metal nanoparticles, silver nanoparticles have been known to have inhibitory and bactericidal effects. The high surface area and high fraction of surface atoms of Ag nanoparticles lead to high antimicrobial activity as compared with bulk silver metal. Hence silver nanoparticles have been chosen to be our core material which can act as an antimicrobial as well as an anticancer agent. In spite of using silver nanoparticles, we need an additional layer to prevent silver from oxidizing and similarly to reduce the usage of silver concentration. Hence we preferred metal—oxide layer to effectively overcome the detrimental effects of silver nanoparticles. Among various semiconductors, TiO₂ nanoparticles are investigated widely due to their significant properties such as photosensitivity, non-toxicity, easy availability, strong oxidizing power, and long-term stability. The photocatalytic properties of TiO₂ have led to extensive research into its potential uses as a disinfectant, antibiotic, biological sensor, tumor cell-killing agent, and gene targeting device. Bulk forms of TiO₂ are generally biologically and chemically inert. The size, shape, and aggregation of titanium dioxide nanoparticles are the important factors in the anticancer activity and *In vivo* toxicological analysis.

3 Characteristic Features of Silver and TiO₂ Nanoparticles in Drug Delivery

Silver nanoparticles usually involve some form of moisture layer that the silver ions are transported through, to create long term protective barrier against bacterial and fungal properties. Silver nanoparticles display a synergistic effect and also a cytotoxic effect on cell viability which have a chief role in antitumor effect. They aid in gathering and transporting drug into the cancer cells and they also obstruct the metabolism of cancer proliferation [2–6]. TiO₂ is a biocompatible material which in nanosized form causes some inflammation effects and confirms the idea that nanomaterials have different properties compared with bulk materials. Some evidence shows that the nano-TiO₂ causes H₂O₂ and hydroxyl free radical formations which results to cell toxicity in mammals. The surface of TiO₂ nanoparticles is highly reactive because of surface defects and such TiO₂ nanoparticles readily bind ligands including dopamine, ascorbic acid and alizarin. The endocytosis of nanoparticles depends on the size, shape and charge of the nanoparticles as well as the cell type being treated. The unique characteristic feature such as small

size and quantum size effect could make silver and TiO₂ nanoparticles suitable for many applications [7–13].

4 Chemical Preparation Technique—Stober Method

Many methods allow preparing particles from solution or from vapour phase. One of the most popular methods is called Stober method. The method is based on the hydrolysis and poly condensation of alkyl compounds in basic (ammonia) alcoholic solutions, therefore on the sol-gel method reactions. The particles size strongly depends on the water and ammonia concentration, but also on the nature of the alcohol used as a solvent. When using alcohols of higher molecular weight, the reaction is slowed down and both median particle size and the spread of the size distribution increased simultaneously. By using the Stober method, it is possible to achieve excellent control of particle size, narrow size distribution and smooth spherical morphology. This method is the extension of sol gel method, where the particles undergo hydrolysis and condensation process. Sol gel processes are mainly classified into three different approaches (i) gelation of solutions of a colloidal powder, (ii) hydrolysis and poly condensation of metal alkoxides or metal salt precursors followed by hyper critical drying of the gels (iii) hydrolysis and poly condensation of metal alkoxides precursor followed by aging and drying under ambient atmosphere [14]. Figure 1 shows the schematic illustration of the Stober synthesis of nanomaterials.

5 Stober Chemistry

Chemistry involved in the sol-gel process is very important for the proper fabrication of desired material. Initial conditions such as pH, temperature, etc., control the extended sol-gel chemistry. The hydrolysis and poly condensation of alkoxides proceed according to the following mechanism,

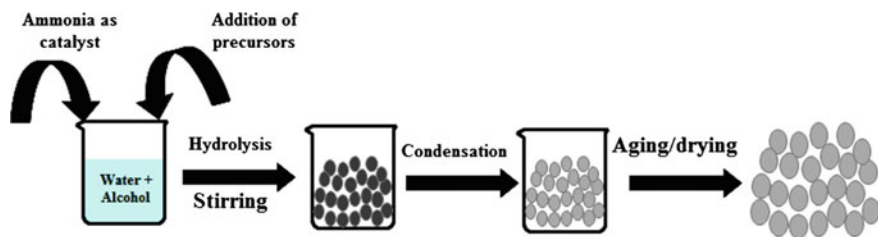


Fig. 1 Schematic illustration of Stober method

Hydrolysis: $M(OR)_n + nH_2O \rightarrow M(OH)_n + nROH$

Condensation: $M(OH)_n + M(OH)_n \rightarrow (OH)_n - 1 M-O-M-(OH)_n - 1 + H_2O$

6 Preparation of Bio-surfactants Induced Ag–TiO₂ Core Shell Nanoparticles

(a) Preparation of Ag nanoparticles

Silver NPs were prepared by the reduction of silver nitrate with Hydrazine monohydrate at RT, according to the method described previously by Lendel and Leopold. Briefly 11.6 mg of $N_2H_4 \cdot H_2O$ was dissolved in 100 ml of distilled water and was mixed with 0.1 M of NaOH. Then 36 ml of the above solution, was added with 10 mM of $AgNO_3$ (4 ml) under gentle stirring at RT. A rapid colour change was observed and finally a clear blackish-yellow Ag NPs was obtained [15].

(b) Preparation of Ag NPs @ biosurfactants

A typical procedure for the synthesis of biosurfactants induced Ag NPs preparation is gives as follows: the prepared Ag NPs were slowly added to 2-propanol ($H_2O/2$ -propanol, ratio maintained at 4:20). Under gentle stirring, ammonia (6 ml, 25 %) and biosurfactants (80 μ l) were added to the above mixture. The mixture was

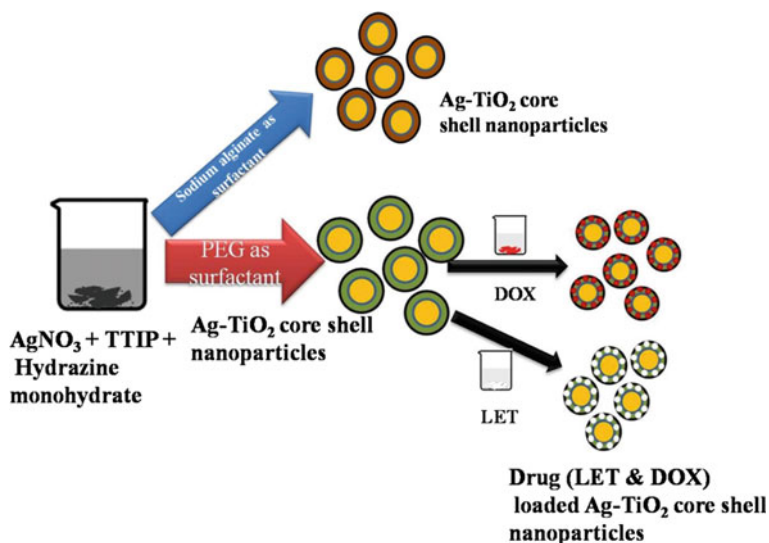


Fig. 2 Schematic diagram of biosurfactants (PEG and sodium alginate) induced Ag–TiO₂ core shell nanoparticles

sonicated for about 15 min to get homogeneous dispersion. Figure 2 shows the schematic diagram of synthesis of pure and drug loaded Ag–TiO₂ core shell nanoparticles.

(c) Preparation of Ag NPs @ biosurfactants @ TiO₂

Aqueous solution of Tween 80 of 0.1 M was dissolved in pre-mixed dispersion of above prepared mixture (core particles). With the above mixed core particles, different concentrations of titanium precursor (0.8, 1.6 and 2.4 ml) dissolved in 2 ml of ethanol was added. The mixture was sonicated for at least 30 min in an ultrasound bath to get homogeneous dispersion. After sonication, the mixture was stirred for 2 h at room temperature. The colour of the solution changed to grey from blackish yellow which confirmed the coating of titanium dioxide over silver nanoparticles. The product was washed with ethanol and water and calcined at 400 °C for 2 h [15].

(d) Anti-cancer drug loading

90–80 mg of Ag–TiO₂ core shell nanoparticles was dissolved in 8 ml of DMSO and 10–20 mg of anticancer drugs (DOX and LET) separately dissolved in 2 ml of DMSO with equivalent molar ratio of TEA. These solutions were mixed and magnetically stirred for 1 h [16]. This solution was poured into 20 ml of distilled water for 10 min to form anticancer drug incorporated nanoparticles. DMSO and free drug was removed by dialysis. The resulting solution was used for analysis or lyophilized.

7 Characterization Techniques

The X-ray diffraction (XRD) recording were carried out at room temperature using a PANalytical X'Pert-Pro diffractometer with Cu K α radiation ($\lambda = 1.5406 \text{ \AA}$) over a scanning interval (2Θ) from 20° to 80°. The average crystallite sizes were estimated using the Scherrer formula from the X-ray line broadening. The infra-red spectrum of the samples was obtained by using a Fourier trans-form infrared (FTIR) spectrometer (Bruker Tensor, Germany). The sample was prepared in a KBr pellet for the investigation within the range of 4000–400 cm⁻¹. The morphology of the Ag–TiO₂ and anticancer drug loaded core shell nanostructures was observed by field emission scanning electron microscopy (FESEM) (FEI Quanta-250 FEG) and Transmission electron microscope (TEM, Hitachi H600) operating at 80 kV. UV-vis spectral analysis was done by using JoscoV-650 spectrophotometer. The chemical composition of the surface layer was determined by X-ray photoelectron spectroscopy (XPS, AXIS165) spectrometer. The stability and charge of the nanoparticles were determined by Zeta potential analyzer. The entrapment efficiency, drug loading and drug releasing profile were calculated using JoscoV-650 UV-vis spectrophotometer.

8 Silver Releasing Tests

A mass of 0.1 g of the product was soaked in 25 ml of Phosphate buffer solution (PBS) in polypropylene bottle at 37 °C and rotated at 300 rpm, for periods of intervals ranging from 1 to 7 days. The liquid was collected on the 1st, 3rd, 6th and 7th days and replaced with fresh Phosphate buffer solution (PBS). At selected intervals, the concentrations of silver ions released from the product into the Phosphate buffer solution (PBS) were measured using UV-vis spectroscopy. The experiments were performed in triplicate to obtain the average value. The samples were analysed and the average and standard deviation with error value were calculated. Statistical analysis was performed by using Microsoft Excel [17].

9 In-Vitro Studies

(a) Antibacterial assay

The strains of *Staphylococcus aureus* bacteria were grown in Luria-Bertania (LB) medium containing 10 g/L tryptone, 5 g/L yeast extract, and 5 g/L NaCl. The bacteria were inoculated in the LB medium in a self regulating thermostat for 8 h at 37 °C. One millilitre original bacterial inoculum was added into 9 ml 0.9 % normal saline and they were diluted into LB broth for 8 h at 37 °C. Once the standard culture was prepared, two methods were used to study the antibacterial activity such as (i) optical density tests and (ii) colony count method [18].

(b) Optical density tests

To examine the bacterial growth rate and to determine the growth curve in the presence of the prepared Ag–TiO₂ core shell nanoparticles, *S. aureus* were grown in 50 ml LB medium as in single agar plate colony supplemented with 0, 20, 40, 60, 80 and 100 µg of Ag–TiO₂ core shell nanoparticles. Growth rates and bacterial concentrations were determined by measuring optical density at 600 nm each 2 h for 24 h at 37 °C (OD of 0.1 corresponds to a concentration of 10⁵ cells) [19].

(c) Colony-counting method

The minimal inhibitory concentrations were measured by plate count method. Viable cell counts were determined by tenfold serial dilution of 1 mL broth culture in phosphate buffer solution (PBS), followed by inoculation of 0.1 mL aliquots on nutrient agar, by incubation of the plates at 37 °C for 24 h prior to colony plate counting. After the incubation, the number of colonies grown on the agar was counted.

(d) Estimation of protein leakage from bacterial cell membranes

Protein leakage from bacterial cells was detected using Lowry's method using bovine serum albumin (BSA) as standard. The concentration of Ag–TiO₂ core shell

nanoparticles was adjusted to 100 µg/ml, and the concentration of bacterial cells was 10⁵ CFU/ml [20]. Each culture was incubated in a shaking incubator at 37 °C for 6 h and 1 ml of culture sample was obtained from each culture. The sample was centrifuged at 4 °C for 30 min at 300 rpm and the supernatant was frozen at −20 °C until assay. The protein content of the supernatant was estimated [21].

(e) In vitro haemolysis analysis of Ag/TiO₂ of core shell nanoparticles

Haemolysis assay was performed using fresh blood of sheep. The erythrocytes were collected by centrifugation at 1500 rpm for 15 min and then washed three times with phosphate buffered saline (PBS) buffer at pH 7.4. The stock dispersion was prepared by mixing 3 ml of centrifuged erythrocytes into 11 ml of PBS. The prepared PEG and sodium alginate induced core shell nanoparticle dispersion were prepared in PBS buffer with above mentioned concentration (100 µg/ml). One hundred microlitre of stock dispersion was added to 1 ml of nanoparticle dispersions. The solutions were mixed and incubated for 4 h at 37 °C in an incubator shaker. The percentage of haemolysis was measured by UV-vis analysis of the supernatant at 394 nm absorbance after centrifugation at 13,000 rpm for 15 min. One millilitre of PBS was used as negative control with 0 % haemolysis and 1 ml of DD H₂O was used as the positive control with 100 % haemolysis. All haemolysis data points were represented as the percentage of the complete haemolysis.

(f) Measurement of drug encapsulation efficiency

Drug entrapment efficiency was determined by centrifuging aqueous dispersion of LET and DOX loaded Ag–TiO₂ core shell nanoparticles at 25,000 rpm for 15 min and measuring the amount of LET and DOX in the supernatant with the help of UV-vis spectrophotometer, absorbance at 240 nm (LET) and 480 nm (DOX). The amount of LET and DOX were subtracted from initial amount of anticancer drug taken to calculate drug entrapment efficiency of nanoparticles [22].

(g) Drug release study

The releasing experiments were carried out in vitro as follows: 2 mg of incorporated nanoparticles were distributed into 10 ml phosphate buffer solution (PBS, 0.1 M, pH 7.4) and this solution was introduced into dialysis membrane tubes. The dialysis membrane was then placed in a 250 ml bottle with 90 ml of PBS solution. This bottle was continuously stirred for 6 h at 37 °C. At specific time intervals (every one hour), 3 ml media was withdrawn to determine drug release by absorbance measurement at wavelength of 240 nm (LET) and 480 nm (DOX); another 3 ml of PBS solution was added to the dialyzed solution to compensate the withdrawn volume [23]. The concentration of released drugs from the nanoparticles into PBS solution was evaluated by UV-vis spectroscopy. Cumulative percentage released at different time points were fitted into different release models: Zero order kinetics, First order kinetics, Higuchi and Korsmeyer-peppas plot. The Correlation coefficient close to unity was taken as order of release.

10 Conclusion

Biosurfactants induced Ag–TiO₂ core shell nanoparticles were prepared by Stober method (extended sol gel method) with titanium (IV)-iso propoxide and silver nitrate as starting precursors. The silver nitrate was chemically reduced to silver nanoparticles with hydrazine monohydrate as reducing agent. The prepared core shell nanoparticles were confirmed by various characterization studies such as FESEM, TEM, XPS and XRD. These analyses showed the formation of core shell structure with Ag in metallic state and TiO₂ in pure anatase phase. Further the influence of prepared core shell nanoparticles on the bacterial properties has been analyzed and the results showed PEG induced core shell nanoparticles had higher activity.

With this core shell nanoparticles, the anticancer drugs has been loaded and its cumulative % release results indicates the zero order kinetics with super case II model, which make the drug to release in a controlled and relaxing manner from the carrier into the targeted site. The interaction between these metal and metal oxide makes it suitable for various fields such as photocatalysis, water purification and mainly focuses its needs in biological field due to its higher efficacy.

References

1. Chaudhuri, R.G., Paira, S.: *Chem. Rev.* **112**, 2373–2433 (2012)
2. Wu, K.C.W., Yamachi, Y., Hong, C.Y., Yang, Y.H., Liang, Y.H., Funastu, T., Tsunoda, M.: *Chem. Commun.* **47**, 5232–5234 (2011)
3. Shi, H., Magaye, R., Castranova, V., Zhao, J.: *Part. Fibre Toxicol.* **10**, 15 (2013)
4. Coronado, D.R., Gattorno, G.R., Espinosa-Pesqueira, M.E., Cab, C., De Cossa, R., Oskam, G.: *Nanotechnology* **19**, 145605 (2008)
5. Bonetta, S., Bonetta, S., Motta, F., Strini, A., Carraro, E.: *AMB Express* **3**, 59 (2013)
6. Thevenot, P., Cho, J., Wavhal, D., Timmons, R.B., Tang, L.: *Nanomed. Nanotechnol. Biol. Med.* **4**, 226–236 (2008)
7. Reidy, B., Haese, A., Luch, A., Dawson, K.A., Lynch, I.: *Material* **6**, 2295–2350 (2013)
8. Asharani, P.V., Mun, G.I., Hande, M.P., Valiyavettill, S.: *ACS Nano* **3**, 279–290 (2009)
9. Tvan, Q.H., Ngugen, V.Q., Le, A.T.: *Adv. Nat. Sci. Nanosci. Nanotechnol* **4**, 033001 (2013)
10. Das, S.K., Bhunia, M.K., Bhaumik, A.: *Dalton Trans.* **39**, 4382–4390 (2010)
11. Li, S., Guoliang, Ye, Chen, G.: *J. Phys. Chem. C* **113**, 4031–4037 (2009)
12. Zhang, H.J., Wen, D.Z.: *Surf. Coat. Technol.* **201**, 5720–5723 (2007)
13. Su, W., Wang, S., Wang, X., Fu, X., Weng, J.: *Surf. Coat. Technol.* **205**, 465–469 (2010)
14. Farooqui, M.D.A., Chauhan, P.S., Krishnamoorthy, P., Shaik, J.: *J. Nanomater. Biostruct.* **5**, 43–49 (2010)
15. Yunqing, W., Lingxin, C., Ping, L.: *Chem.Eur. J.* **18**, 5935–5943 (2012)
16. Jeong, Y.-I.L., Chung, K.-C., Choi, K.C.: *Arch. Pharm. Res.* **34**, 159–167 (2011)
17. Nithyadevi, D., Sureshkumar, P., Mangalaraj, D., Ponpandian, N., Viswanathan, C., Meena, P.: *Appl. Surf. Sci.* **327**, 504–516 (2015)
18. Kim, J., Sungeun, K., Kim, J., Jongchan, L., Yoon, J.: *Korean Soc. Environ. Eng.* **27**, 771–776 (2005)
19. Wang, J.X., Wen, L.X., Wang, Z.H., Chen, J.F.: *Mater. Chem. Phys.* **96**, 90–97 (2006)

20. Bradford, M.M.: *Anal. Biochem.* **72**, 248–254 (1976)
21. Guerlavy, P., Izac, V., Tholozan, J.L.: *Curr. Microbiol.* **36**, 131–135 (1998)
22. Jeong, Y.-I.L., Choi, K.C., Song, C.E.: *Arch. Pharm. Res.* **29**, 712–719 (2006)
23. Noveen, K., Aravind, G., Sumit, S., Prashanthi, P.: *Int. J. Pharm. Pharm. Sci.* **5**, 615–621 (2013)

Recent Trends in Materials Science and Applications
Nanomaterials, Crystal Growth, Thin films, Quantum
Dots, & Spectroscopy (Proceedings ICRTMSA 2016)

Ebenazar, J. (Ed.)

2017, XXXIII, 735 p. 396 illus., 295 illus. in color.,

Hardcover

ISBN: 978-3-319-44889-3